Optimal Fault Predictors for Arc-Type Faults in Radial and Meshed Alternating Current Distribution Systems

G. B. Weyrich Morris, *Student Member, IEEE,* E. Castillo-Guerra, *Senior Member, IEEE* , A. M. Sharaf, *Senior Member, IEEE* and M. Stevenson, *Senior Member, IEEE*

***Abstract*—Efficient and reliable linear and nonlinear fault diagnostic systems are of vital importance in modern utility power grids as quick, accurate detection of faults can assist in preventing system failures that cause economic loss and endanger human or animal life. The foundation of any fault diagnostic system is its set of predictors; robust predictors naturally lead to a reliable system. This work fills the need for a deep investigation into reliable fault detection predictors. Novel harmonic-based fault predictors are developed for diagnosis of fault condition in both radial and meshed type AC distribution systems, with four fault classification groups (bolted fault, high impedance non-linear fault, linear fault, and a no-fault classification). These new fault predictors are optimized and rigourously tested aganist earlier fault predictors using existing fault models and known statistical methods in both noiseless and noisy conditions.**

***Index Terms*—Fault diagnosis, harmonic analysis, intelligent sensors, network fault diagnosis, power distribution faults.**

I. Introduction

IN the modern, overburdened electric utility power grid, the High Impedance arc-type Fault (HIF) and related faults which do not immediately alert traditional over-current or ground type protection systems [1]-[3] can subtly drain power from the intended load, placing additional stress on already highly-taxed distribution systems, and posing safety concerns. This causes economic and environmental loss for the extra power that must be delivered, and endangers the public and wildlife in the incidence of downed lines or low impedance paths. Accordingly, effort must be invested in developing effective fault diagnostic systems which work quickly and efficiently to reliably detect faults before they pose safety hazards or cause environmental or property damage. This is particularly important in sources of renewable energy such as wind turbines or power cells where such faults can cause voltage and current fluctuations that can damage sensitive equipment or produce severe power losses.

One of the most fundamental aspects of designing a reliable fault diagnostic relay is the choice of fault predictors; carefully choosing predictors which offer the best performance in terms of reliability, efficiency and calculation burden will help lead to an efficient, reliable detection system. Previously discovered predictors [3]-[8] have been shown to be effective in small-scale tests using computationally intensive neural network or similar pattern recognition algorithms, however these predictors show high correlation, indicating the existance of redundant information. A need therefore exists to scrutinize these predictors or to define new ones that optimize the performance of fault diagnosis systems and minimize the computational burden, providing efficient and reliable real-time implementations. This work relies on a careful study of the data corresponding to bolted, linear and HIF faults, developing a new, optimized set of features from a signal processing perspective. The performance of the developed predictors are compared to previously reported algorithms [3].

II. Models and Faults

Three different common fault types (bolted, linear, and HIF) and one control group (no fault) were analyzed on two distribution systems: radial and meshed distribution systems. Each fault has certain distinct characteristics: the bolted fault is a shunted condition where effectively no impedance exists at the fault location; the high impedance arc-type fault (HIF) is a non-linear fault modeled by

$$R_f = R_{fo} + R_{fl}\,\alpha\left(\frac{i_f}{i_{fo}}\right)^{\beta}, \qquad (1)$$

[8], [9]; the linear fault is a low-current fault, like the HIF, but linear in nature; and the no fault control condition is where the circuit operates normally [8]. All faults were tested on the equivalent, previously developed models of both the radial distribution feeder (Fig. 1 A) and the meshed distribution system (Fig. 1 B).

The eight resultant fault state models [8] were each simulated 256 times with a set of random fault parameters and a set of fixed system parameters (Table I). All signals were simulated with a sampling rate of 12kHz for a duration of 0.1s

This work was supported by the Natural Sciences and Engineering Research Council of Canada.

G. B. Weyrich Morris is an Undergraduate Electrical Engineering student at the University of New Brunswick, Fredericton, NB E3B 5A3 Canada (e-mail: G.B.Morris@unb.ca).

E. Castillo Guerra is an Assistant Professor with the Department of Electrical and Computer Engineering at the University of New Brunswick (e-mail: ecastill@unb.ca).

A. M. Sharaf is a Professor with the Department of Electrical and Computer Engineering at the University of New Brunswick (e-mail: sharaf@unb.ca).

M. Stevenson is a Professor with the Department of Electrical and Computer Engineering at the University of New Brunswick (e-mail: stevenso@unb.ca).

1. R_f is the arc, non-linear fault resistance, i_f is fault current, R_{fo} is 100Ω, R_{fl} is usually high, between 50Ω and 150Ω, α is selected between 0.3 and 0.7, i_{fo} is selected at 70A, and β is equal to 2.

for each of the four circuit parameters investigated: voltage, current, impedance and power. (N.B. Only two quantities need be measured, namely voltage and current; the other two can be thence calculated.) This simulation was performed twice to produce two sets of data, each having 1024 different fault cases; one data set was used for training, and the other for testing the fault diagnosis system.

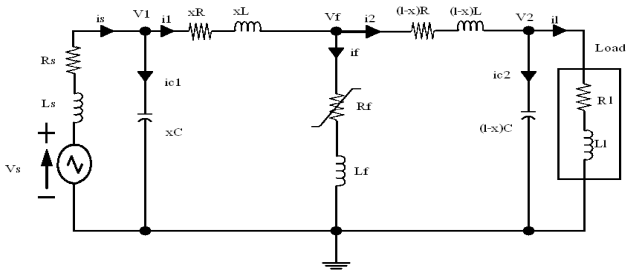

Fig. 1 A.Single phase equivalent model of the radial system with HIF at location x. All other fault types follow from this diagram [6].

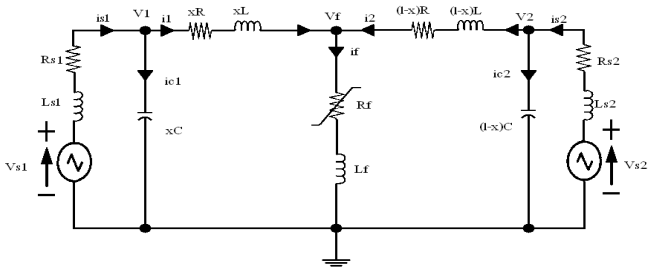

Fig. 1 B.Single phase equivalent model of the meshed system with HIF at location x. All other fault types follow from this diagram [7].

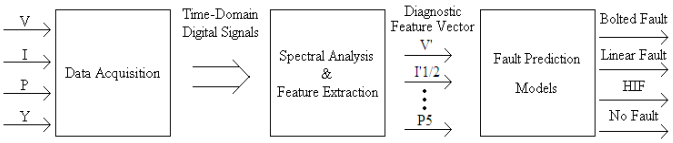

Fig. 2. Proposed diagnostic relaying scheme.

III. Frequency Domain Analysis

In accord with previous research in the area of fault detection and recognition of arc-type non-linear HIF faults [1]-[9], the signal analysis was performed in the frequency domain, by means of the Fast Fourier Transform (FFT), which effectively reveals the identifying patterns of the different faults investigated. Nine new measures were developed from extensive observation of the frequency domain signals. A complete list of old and new predictors can be found in Table VI in the Appendix.

The single new predictor taken from the voltage signal was the magnitude of the first harmonic divided by the magnitude of the trough that immediately follows it (as indicated in the top left plot of Fig. 3), henceforth denoted by V'. Three of the four faults have very similar values for the first voltage harmonic, with the Bolted Fault showing a significantly lower first harmonic than the other three. This is not readily apparent in Fig. 3 due to the normalization process, but it can be appreciated upon examination of Table II.

Table I
Fault Parameters Ranges for Both Radial and Meshed Fault Conditions.

Fault Parameter	Range of Values
Fault Inductance, L_f	1.0-5.0 mH
Non-Linear Resistance Parameter, R_{fl}	50-150 Ω
Non-Linear Resistance Parameter, α	0.3-0.7
Radial Fault Location, x	2.5-22.5 km
Radial Load Resistance, R_l	72-144 Ω
Radial Load Inductance, L_l	0.1719-0.3438 H
Meshed Fault Location, x	5-45 km
Phase Angle between Meshed Sources, φ	5-20°
Source Resistance, R_s	0.7 Ω
Source Inductance, L_s	7 mH
Source Frequency, f_s	60 Hz
Line Resistance, R_l	0.25 Ω/km
Line Inductance, L_l	0.99472 mH/km
Line Capacitance, C_l	11.17 nF/km
Radial Line Length, l_R	25 km
Meshed Line Length, L_M	50 km
Radial Source Voltage, V_R	25 kV
Meshed Source Voltage, V_M	500 kV

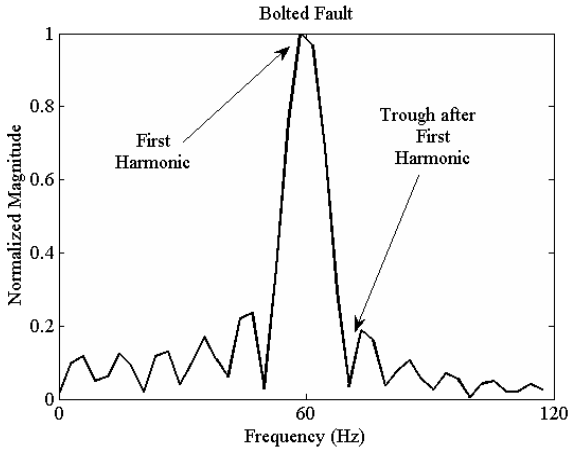

Fig. 3. Normalized spectral magnitude of the voltage signal for each fault type. Plot indicates the frequencies used to calculate the predictor V'.

Four predictors were taken from the current signal, they were: the ratios of the first to the second harmonic, the third to the second, the fifth to the third, and the first to the third (Fig.4), denoted as I'1/2, I'3/2, I'5/3, and I'1/3, respectively. The peculiar nature of the HIF can be observed in the top right plot of Fig. 4.

Two predictors were taken from the admittance spectral magnitude. The first one, shown in Fig. 5, is the ratio of the first maximum to the fifth maximum (the "fifth maximum" specifically being the maximum that occurs directly after 500 Hz). The second is the ratio between the magnitude of the DC

value of the normalized admittance spectrum and the magnitude of the apex of the quadratic curve fit to the first quarter of the FFT, as illustrated in Fig. 6. The two admittance ratios are denoted by ASR, and ALR respectively.

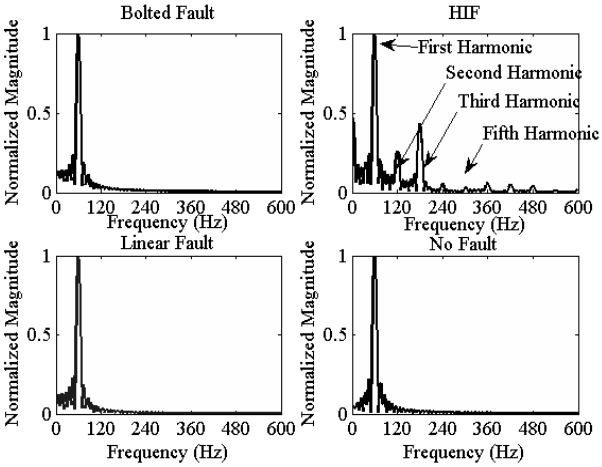

Fig. 4. Normalized spectral magnitude of the current signal for each fault type. Top right plot indicates the frequencies used to calculate the predictors I'.

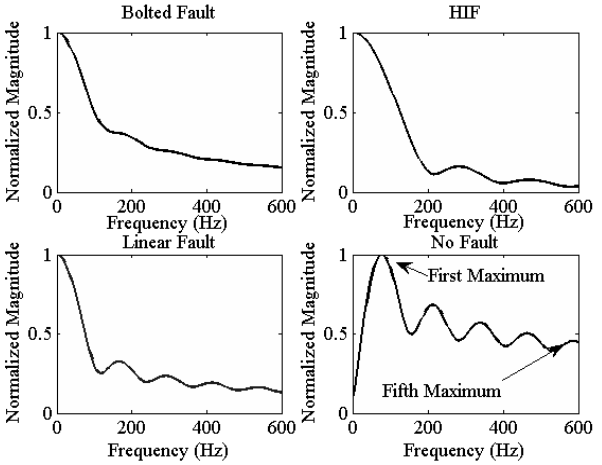

Fig. 5. Normalized spectral magnitude of the admittance signal for each fault type. Bottom right plot indicates the frequencies used to calculate the predictors.

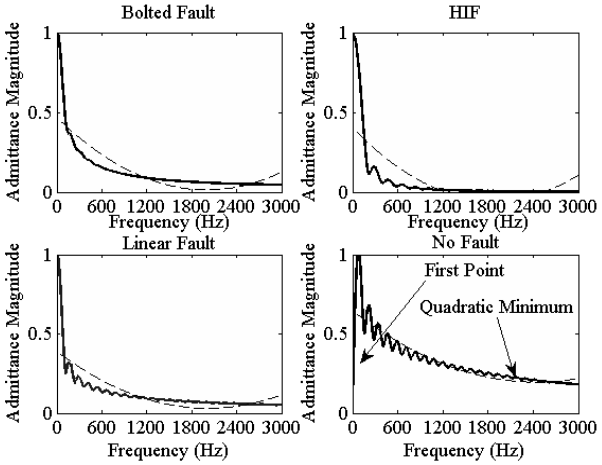

Fig. 6. A longer view of the normalized admittance spectral magnitudes. Each plot shows the quadratic fit (dashed line) used to estimated the second spectral descriptor.

The admittance signal posed certain challenges on account of its unusual nature in the time domain; it is rife with discontinuities. In order to extract the most meaningful information, the time signal was analyzed only up to the first discontinuity (Fig. 7). Analyzing more or less than this amount tended to cause data from different groups or faults to overlap and become less distinct.

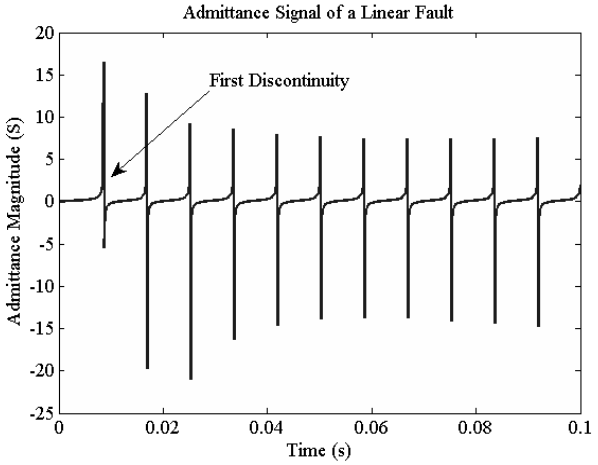

Fig. 7. Time domain representation of the Admittance signal.

Two predictors were taken from the normalized power spectrum; the ratio of the first to the second and the third to the second harmonics (Fig. 8), denoted by P'1/2, and P'3/2 respectively.

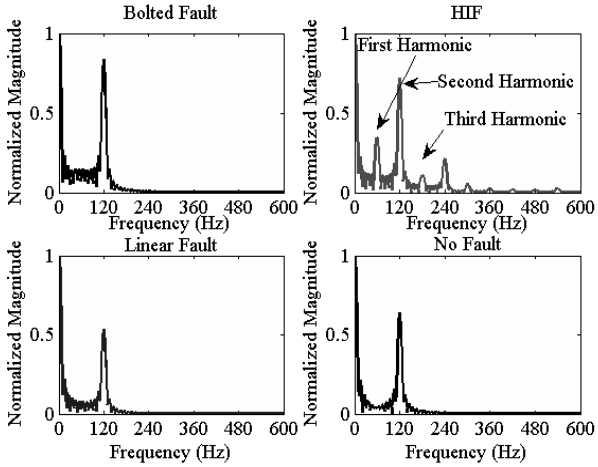

Fig. 8. Normalized spectral magnitude of the power signal for each fault type. Top right plot indicates the harmonics used to calculate the predictors.

Six previously developed measurements [3], [6] were also taken from each case. These were the absolute magnitudes of the third and fifth harmonics from the normalized voltage, current, and power spectra. These are denoted as V3, V5, I3, I5, P3, and P5.

To obtain noisy cases the original, clean simulated data was summed with Gaussian noise having zero mean and standard deviation equal to 10% of the signal amplitude range. This is very rigorous considering the quality of modern power grids.

The statistics of each measurement from the radial system

are shown in Table II. Only statistics from the clean, radial system are shown to familiarize the reader with the predictors and their nature; the optimization process involved several more tables of this type, specifically for the noisy radial system and for both the clean and noisy meshed system. It should be noted that all predictors were normalized prior to linear discriminant analysis.

TABLE II
KEY STATISTICS OF PREDICTORS IN A RADIAL SYSTEM WITH NO NOISE[2]

Predictor	Bolted Fault		HIF		Linear Fault		No Fault	
	$\bar{x}$	s.d.	$\bar{x}$	s.d	$\bar{x}$	s.d.	$\bar{x}$	s.d.
V'	30.613	1.556	34.889	0.0454	34.905	0.0432	34.916	0.0391
I'1/2	21.330	0.179	4.4104	1.3308	24.948	0.366	23.089	0.680
I'3/2	0.45181	0.00317	1.8281	0.3700	0.34416	0.0073	0.4145	0.0172
I'5/3	0.50185	0.00241	0.10344	0.03333	0.39322	0.0210	0.4677	0.0194
I'1/3	47.214	0.724	2.3673	0.2261	72.541	2.480	55.860	4.032
ASR	0.17911	0.02148	0.07662	0.01507	0.15774	0.0162	0.2779	0.0286
ALR	0.05941	0.01193	0.01237	0.01000	0.06461	0.0081	0.1361	0.0167
P'1/2	33.165	1.032	6.682	2.148	34.710	0.388	32.644	0.117
P'3/2	0.36515	0.02960	1.9369	0.3744	0.31834	0.0089	0.3194	0.0087
V3	468.99	127.17	836.31	3.05	833.94	3.25	839.93	2.70
V5	86.09	30.10	282.98	7.01	191.67	1.93	193.62	1.17
I3	275.02	107.18	8.5313	0.8739	14.360	1.582	10.339	1.596
I5	134.80	53.46	68.639	11.699	4.2449	0.6636	4.5955	0.9099
P3	24221	3461	1098.4	243.5	3532.3	313.7	1726.5	217.8
P5	2216.3	278.1	999.62	130.01	232.87	26.90	164.75	22.69

IV. OPTIMIZATION AND TESTING

Once the predictors had been determined it became necessary to analyze their capacity to differentiate the studied faults, and select the best predictor or combination of predictors that would maximize the classification performance. This was accomplished using a combination of statistical tools, most notably variable clustering and linear discriminant analysis (LDA).

Linear discriminant analysis is an established statistical methhod for feature classification [10]. The work in this paper was based on the assumptions that all fault classes were equally probable and that the probability densities of the feature vectors are multivariate normal with a different mean vector for each fault class but the same covariance matrix for each fault class. Under these assumptions, a feature vector was assigned to the fault class whose mean vector is closest (in terms of the Mahalanobis distance) to the feature vector. The mean vector for any class is calculated as the average of the class feature vectors in the training set; whereas the covariance matrix used in the Mahalanobis distance measure is calculated as the covariance of all feature vectors in the training set. Once all input vectors have been classified by the LDA, the classifications or diagnoses assigned were compared to the actual fault types of each of the input vectors. The ratio of correct classifications to total cases is refered to in this paper as the "classification ratio".

TABLE III
RESULTS OF LINEAR DISCRIMINANT ANALYSIS WITH CROSSCHECKING PERFOMRED ON MOST RELEVANT COMBINATIONS OF PREDICTORS IN A RADIAL SYSTEM

Predictors Used	Proportion Classified Correctly	
	Clean	Noisy
I'(1/2, 3/2, 5/3)	0.959	0.633
I'(1/2, 3/2, 5/3, 1/3), P'(2/3, 4/3)	0.990	0.646
I'(1/2, 3/2, 5/3, 1/3), P'(2/3, 4/3), V'	0.999	0.652
A(SR, LR)	0.951	0.414
A(SR, LR), I'(1/2, 3/2, 1/3)	1.000	0.637
[All New Predictors]	0.999	0.649
P(3, 5)	1.000	0.997
P(3, 5), I5	1.000	1.000
[All Old Predictors]	0.998	1.000

TABLE IV
RESULTS OF LINEAR DISCRIMINANT ANALYSIS WITH CROSSCHECKING PERFOMRED ON MOST RELEVANT COMBINATIONS OF PREDICTORS IN A MESHED SYSTEM

Predictors Used	Proportion Classified Correctly	
	Clean	Noisy
I'5/3	0.751	0.402
I'(5/3, 1/3)	0.954	0.574
I'(5/3, 1/3), V', ASR	0.974	0.586
I'(3/2, 5/3, 1/3), V', ASR	0.974	0.588
I'(1/2, 3/2, 5/3, 1/3), P'(2/3, 4/3), V'	0.962	0.633
[All New Predictors]	0.967	0.649
P(3, 5)	0.779	0.714
P3, I5	0.900	0.850
V5, I5, P3	0.904	0.816
V5, I(3, 5), P3	0.905	0.824
[All Old Predictors]	0.900	0.775
I'(5/3, 1/3), V', ASR, V5, I5, P3	0.968	0.810
I'(1/2, 5/3, 1/3,), A(SR, LR), P'(2/3, 4/3), V5, I5, P3	0.977	0.822
[All Predictors]	0.988	0.826

The classification results of the most relevant combinations of variables are shown in Tables III and IV. It is observed that the best combination for both the clean and noisy radial systems is P(3, 5), and I5 with a classification ratio of 100%. For clean, meshed system, the best combination is the entire set of new and old predictors together, giving a classification ratio of 98.8%. However, considering the performance and efficiency criteria, the combination of I'(5/3, 1/3), V', and ASR provide

2. Mean is denoted by $\bar{x}$, standard deviation by "s.d."

the best compromise, with a classification ratio of 97.4%. For the noisy, meshed system the best combination is P3, and I5, giving a classification ratio of 85.0%.

The best predictors from each system were used to implement a new, more realistic LDA analysis. In this case, the crosschecking technique, which only uses one set for both training and testing was replaced with a traditional two set approach (one set for training and one set for testing). This approach assumes that the training set would contain information that is statistically significant for each class and the results will apply to the rest of the data or any randomly collected field data. The results are shown in Table V.

TABLE V
RESULTS OF LINEAR DISCRIMINATION PERFORMED ON ONE HALF OF THE DATA SET USING THE BEST NEW AND OLD PREDICTORS FOR BOTH NOISY AND NOISELESS CONDITIONS

System Properties	Predictors Used	Proportion Classified Correctly				
		Bolted Fault	HIF	Linear Fault	No Fault	Total
Clean, Radial	A(SR, LR), I'(1/2, 3/2, 1/3)	1.0000	1.0000	1.0000	1.0000	1.0000
	P(3, 5)	1.0000	1.0000	1.0000	1.0000	1.0000
Noisy, Radial	I'(1/2, 3/2, 5/3, 1/3), P'(2/3, 4/3), V'	0.7500	1.0000	0.5469	0.3438	0.6602
	P(3, 5), I5	1.0000	1.0000	1.0000	1.0000	1.0000
Clean, Meshed	I'(5/3, 1/3), V', ASR	1.0000	1.0000	0.8672	1.0000	0.9668
	V5, I(3, 5), P3	0.9688	0.9766	0.9219	0.6797	0.8867
Noisy, Meshed	[All New Predictors]	0.4609	0.9922	0.6484	0.4844	0.6465
	P3, I5	0.9922	0.9844	0.8750	0.5547	0.8516

V. CONCLUSION

It can be observed that optimal combinations of new fault predictors perform equally well as old reported predictors in the case of the Radial Model, and outperform old predictors, in the case of the Meshed Model, in low noise conditions. However their efficacy was reduced when the high noise (effectively 20%) was introduced in the generated signals. This is caused by the relative nature of the new features compared to the absolute nature of old ones; that is while the old predictors are based on absolute magnitudes, the new predictors are ratios of those magnitudes, which effectively doubles the noise perturbations present in the result. The situation is not as dire as it may seem for the new predictors, however, as the level of noise introduced in this study was substantially higher than the average noise level which would be experienced in a real distribution system [11], and served to offer as much contrast as possible between the old and the new predictors. It should also be noted that for most of the sets, the condition classified the most poorly tended to be the No Fault condition, which may cause problems with false alarms and will be studied in the next step of this research. It should also be noted that the models used to generate the fault signals did not consider some practical grid parameters that would further compromise the discrimination among the studied fault groups. The inclusion in the generation models of variable impedance in the power source, variable transmission line capacity and var-iable load capacity may necessitate the use of non-linear discrimination techniques.

Ultimately, however, it has been shown that the correct combinations of predictors are capable of accurately predicting faults in low noise environments using means as simple as the linear discriminant function. This method yielded correct predictions for almost 97% of the cases in radial and meshed models, and indicates that with a more earnest focus on predictors non-linear pattern recognition techniques may be unnecessary in modern fault diagnostics. This paper was conceived to serve as a footing from which to develop a more complete set of robust, efficient fault predictors for fault detection devices. It is hoped that more interest will be taken in the foundation of fault diagnosis systems, the predictors, leading to more elegant, efficient, and robust diagnostics.

VI. APPENDIX

TABLE VI
A COMPLETE LIST OF PREDICTORS EXAMINED IN THIS PAPER

Predictor	Definition
New Predictors	
V'	Ratio of the first voltage harmonic to the dip or trough that occurs directly after it.
I'1/2	Ratio of the first current harmonic to the second.
I'3/2	Ratio of the third current harmonic to the second.
I'5/3	Ratio of the fifth current harmonic to the third.
I'1/3	Ratio of the first current harmonic to the third.
ASR	Ratio of the first maximum in the normalized admittance spectral magnitude to the maximum occuring directly after 500Hz.
ALR	Ratio of the first point of the admittance spectral magintude to the point occuring at the apex of a quadratic fit to the first quarter of the normalized spectral magnitude.
P'1/2	Ratio of the first power harmonic to the second.
P'3/2	Ratio of the third power harmonic to the second.
Old Predictors	
V3	Magnitude of the third voltage harmonic.
V5	Magintude of the fifth voltage harmonic.
I3	Magnitude of the third current harmonic.
I5	Magnitude of the fifth current harmonic.
P3	Magnitude of the third power harmonic.
P5	Magnitude of the fifth power harmonic.

VII. References

[1] A. M. Sharaf, L. A. Snider, and K. Debnath, "A Third Harmonic Sequence ANN Based Detection Scheme for High Impedance Faults," in *Proc. Sept. 1993 IEEE Elec. & Comp. Eng., 1993. Canadian Conf. on*, pp. 802-806.

[2] A. M. Sharaf, R.M. El-Shrakawy, R.Al-Fatih, and M. Al-Ketbi, "High Impedance Fault Detection On Radial Distribution and Utilization Systems", *Proc. of the IEEE-CCECE Conf. 1996*.

[3] A. M. Sharaf and Syed M. Atif Saleem, "High impedance fault detection using a neural network based relaying scheme", in *Proc. MEPCON-2003*, Shebin El-Kom, Egypt, Dec 18-25, 2003.

[4] A. M. Sharaf, L. A. Snider, and K. Debnath, "A Neural Network Based Relaying Scheme for Distribution System High Impedance Fault Detection," *Proc. ANNs & Expert Systems, 1993, First New Zealand Two-Stream Conf.* on, pp. 321-324.

[5] M. M. Eissa, G. M. A. Sowilam, and A. M. Sharaf, "A New Protection Detection Technique for High Impedance Fault Using Neural Network," in *Proc. July 2006 IEEE Power Eng. 2006 Large Eng. Systems Conf. on*, pp. 146-151.

[6] A. M. Sharaf, and Guosheng Wang, "High Impedance Fault Detection Using Feature-Pattern Based Relaying," in *Proc. Sept. 2003 Transmission & Distribution Conf. & Expo.,* pp. 222-226, vol. 1.

[7] A. M. Sharaf, and Guosheng Wang, "High Impedance Fault Detection Using Low-Order Pattern Harmonic Detection," in *Proc. Sept. 2004 Elec., Electronic, & Comp. Eng., 2004. ICEEC '04. 2004 Int'l Conf. on.,* pp. 883-886.

[8] S. M. Atif Saleem, "Artificial Intelligence AI-Based Detection Schemes for Arc-Type High Impedance Faults," M.Sc.Eng. thesis, Dept. Elec. Comp. Eng., Univ. New Brunswick, Fredericton, NB, Canada, 2004.

[9] A. M. Sharaf, and S. I. Abu-Azab, "A Smart Relaying Scheme for High Impedance Faults in Distribution and Utilization Networks," in *Proc. IEEE 2000 Elec. & Comp. Eng. Canadian Conf. on*, pp. 740-744, vol. 2.

[10] R.O. Duda, P.E. Hart, and D.G. Stork, *Pattern Classification*, second edition, John Wiley & Sons, 2001.

[11] J. B. O'Neal Jr., "Substation Noise at Distribution-Line Communication Frequencies," in *Electromagnetic Compatability, IEEE Transactions on*, Vol. 30, Iss. 1, pp. 71-77, Center for Commun. & Signal Process., N. Carolina State Univ., Raleigh, NC, Feb. 1988.

VIII. Biographies

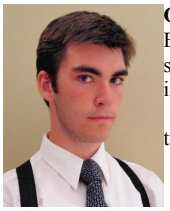

Gregory Weyrich Morris was born in Fredericton, New Brunswick, Canada on 13 December, 1988. He is currently studying for his Undergraduate Degree in Electrical Engineering at the University of New Brunswick.

His technical interests include power and aerospace technologies.

Eduardo Castillo-Guerra obtained his B.Sc. degree in electrical engineering from the Central University of Las Villas (UCLV) in 1992 and his M.Sc. degree in telecommunication from the same university in 1996. He completed his Ph.D. in Electrical Engineering at the University of New Brunswick (UNB) in 2003.

He joined the Center for Studies on Electronics and Information Technology at UCLV in 2003 and received a postdoctoral fellowship with the Institute of Biomedical Engineering at UNB in 2005. He joined the Department of Electrical and Computer Engineering at UNB in 2006 where he is currently an assistant professor.

His research interests include pattern recognition, digital signal and speech processing, digital system design and secure communications.

Adel Sharaf obtained his B.Sc. degree in Electrical Engineering from Cairo University in 1971. He completed an MSc degree in Electrical engineering in 1976 and PhD degree in 1979 from the University of Manitoba, Canada. He joined the University of New Brunswick in 1981 to start a tenure-track academic career as an Assistant professor and he was promoted to Associate Professor in 1983, awarded tenure in 1986, and the full professorship in 1987.

His research interests include Power Systems and Electrochnology, A.I., Multimedia/Internet enhanced Learning, and Pollution Abatement Devices and Systems.

Maryhelen Stevenson (S'78-M'84-SM'07) received the B.E.E. degree from the Georgia Institute of Technology in 1983, and the M.S. and Ph.D. degrees in Electrical Engineering from Stanford University in 1984 and 1991 respectively.

She was a member of the Technical Staff at Hughes Aircraft Company in Fullerton, California from 1983 to 1989. Since 1990, she has been at the University of New Brunswick in Canada where she is currently a Professor of Electrical and Computer Engineering.

Her research intersests include pattern recognition, speech processing, adaptive signal processing, and neural networks.